

# Geometries, stabilities, and reactions of carbon clusters: Towards a microscopic theory of fullerene formation

Yusuke Ueno and Susumu Saito

*Department of Physics, Tokyo Institute of Technology, 2-12-1 Oh-okayama, Meguro-ku, Tokyo 152-8551, Japan*

(Received 2 November 2007; published 1 February 2008)

To clarify the microscopic formation process of  $C_{60}$  and other fullerenes, we study the geometries and energetics of small carbon clusters and the reaction between carbon clusters using the long-range transferable tight-binding model parametrized by Omata *et al.* (Omata TB), the local-density-approximation (LDA) in the framework of the density-functional theory, and the constant-temperature molecular dynamics combined with Omata-TB (Omata TBMD). From the LDA geometry-optimization study, we find that the binding energy per atom of the  $C_{10}$  ring is 0.4 eV/atom larger than that of the  $C_{10}$  chain. This energetic preference of a ring to a chain in  $C_{10}$  is most prominent among all  $C_n$  clusters studied ( $5 \leq n \leq 17$ ). Moreover, the study of *sp*-hybridized small carbon clusters with Omata TBMD reveals that  $C_{10}$  is the smallest stable ring at the temperature of 2000 K, which can explain the high abundance of  $C_{10}$  in the experimental  $C_n^-$  mass spectra. From the remarkable stability of the  $C_{10}$  ring as well as from its high abundance, it is considered that the *sp*-hybridized  $C_{10}$  ring should play a role of major constituent units of larger clusters and fullerenes. Therefore we perform various sets of simulations of reactions between carbon clusters possessing the C atoms in multiples of 10,  $C_{10m} + C_{10n}$  ( $m+n=2,3,4,5,6$ ,  $m \geq n \geq 1$ ), at several temperatures with Omata TBMD. As a result, it is found that, in most cases studied,  $C_{20}$  and  $C_{30}$  clusters possess the  $sp^2$ -hybridized planar geometries, while  $C_{40}$ ,  $C_{50}$ , and  $C_{60}$  take the  $sp^2$ -hybridized “fullerenelike” closed-cage geometries. These  $C_{40}$ ,  $C_{50}$ , and  $C_{60}$  cages can be formed at as low as 1500 K, which is in good accord with the experimental temperature of fullerene formation. In a few cases, even the  $C_{30}$  cluster is found to take the cage structure. These results are in good accord with the experimental results of the gas ion chromatography. The straightforward growth process from the *sp*-hybridized ring to the  $sp^2$ -hybridized plane and that from the  $sp^2$ -hybridized plane to the  $sp^2$ -hybridized fullerenelike cage revealed in the present study are considered to be the main road of the formation of fullerenes. Finally, the study of structural stabilities of cage geometries obtained through the reaction between a fullerenelike cage ( $C_{40}$ ) or a symmetrical fullerene ( $D_{5h} C_{50}$  or  $I_h C_{60}$ ) and a carbon cluster ( $C_{10}$  or  $C_{12}$ ) at various temperatures with Omata TBMD indicates that  $C_{2n}$  fullerenelike cages larger than  $C_{60}$  tend to decay into  $C_{2n-2}$  through the  $C_2$  loss process at the higher rate than  $C_{60}$  or smaller fullerenelike cages. Therefore this  $C_2$  loss process is considered to be one of the most important processes leading to the extreme abundance of  $C_{60}$ .

DOI: [10.1103/PhysRevB.77.085403](https://doi.org/10.1103/PhysRevB.77.085403)

PACS number(s): 73.61.Wp, 61.46.Bc, 31.15.E-, 31.15.xv

## I. INTRODUCTION

The interesting proposal of the truncated-icosahedral structure of  $C_{60}$  named “buckminsterfullerene”<sup>1</sup> and its macroscopic production by resistive heating of graphite<sup>2</sup> stimulated the intensive research of a new form of carbon possessing *zero-dimensional*  $sp^2$  covalent-bond network. Now, not only  $C_{60}$  but also other carbon clusters with the  $sp^2$ -hybridized closed-cage geometries consisting of pentagons and hexagons are called “fullerenes.” In particular, the various physical and chemical properties of the  $C_{60}$  fullerene have been revealed. The  $C_{60}$  fullerenes condensed via weak dispersive force give semiconducting solid,<sup>2-4</sup> the third form of crystalline carbon next to insulating diamond and metallic graphite. This solid  $C_{60}$  is found to show superconductivity by potassium doping,<sup>5</sup> and transforms into one- or two-dimensional polymer under high pressure and temperature.<sup>6,7</sup> Also, a  $C_{60}$  fullerene can encapsulate atoms or molecules into its hollow space.<sup>8,9</sup> In addition, larger fullerenes such as  $C_{70}$ ,  $C_{76}$ ,  $C_{78}$ ,  $C_{82}$ , and  $C_{84}$ , etc., have been extracted from carbon soot.<sup>10,11</sup> However, the reason why  $C_{60}$  is by far the most abundant fullerene in carbon soot still remains unrevealed. Evidently the  $C_{60}$  fullerene is not energetically the

most stable cluster among various carbon clusters in soot. Actually, larger fullerenes, such as  $C_{70}$  and  $C_{84}$ , have larger binding energies per atom than  $C_{60}$ .<sup>12,13</sup> Hence the  $C_{60}$  fullerene should be energetically less stable than larger fullerenes. Nevertheless,  $C_{70}$  is the second most abundant fullerene,<sup>1</sup> and  $C_{84}$  the third. Besides, the production yields of  $C_{70}$  and  $C_{84}$  are much lower than that of  $C_{60}$ . These facts imply the *unimportance* of the binding energy for the preferential productions of  $C_{60}$  fullerenes. Hence to elucidate the “mystery” that  $C_{60}$ , energetically the least stable fullerene in soot, is the most abundant fullerene, one has to unveil the microscopic formation process of fullerenes.

On one hand, the speculative rule in the synthesis of fullerenes, the so-called isolated-pentagon rule (IPR), which means that two or three pentagons are not adjacent in the C-C bond network of fullerenes,<sup>14</sup> is known to be satisfied in the extractable empty fullerenes. In fullerenes smaller than  $C_{70}$ , the IPR can never be satisfied except for  $C_{60}$ . Therefore  $C_{60}$  is the smallest IPR-satisfying fullerene, and  $C_{70}$  is the second smallest. This may reflect that IPR-breaking fullerenes are more reactive than IPR-satisfying ones.<sup>15</sup> Actually, from our previous density-functional study,<sup>16</sup> it has been quantitatively confirmed that the IPR-breaking

fullerene  $C_{50}$  is much more reactive than the IPR-satisfying fullerenes  $C_{60}$  and  $C_{70}$ . More importantly,  $C_{70}$  has been found to be more reactive than  $C_{60}$ . Therefore reactivities of fullerene should be the keys to explaining the high relative abundance of  $C_{60}$  in carbon soot. On the other hand, the low reactivity of  $C_{60}$  itself alone does not explain its *absolute* high abundance, i.e., the high conversion rate of graphite into  $C_{60}$  in the fullerene production process, which is known to be as high as several ten percent.<sup>17,18</sup>

There have been various attempts to fathom the mystery of the formation process of fullerenes. Some of the proposed fullerene formation models are well known: “pentagon road” where the curling of graphitic sheets through the incorporation of pentagons forms fullerenes,<sup>19</sup> “fullerene road” where small fullerenes grow into larger ones through sequential  $C_2$  additions,<sup>20</sup> and the “ring stacking model” where the fullerenes are formed by sequential stacking of carbon rings.<sup>21</sup> Also, several theoretical studies of the microscopic formation process of fullerenes using the molecular dynamics (MD) method were performed. Successful MD *computational synthesis* of  $I_h C_{60}$  and  $D_{5h} C_{70}$  from “fullerenelike”  $C_{60}$  and  $C_{70}$  closed cages, which are also the products of the MD simulation process from gas-phase C atoms, using the empirical interatomic model potential, has been reported.<sup>22,23</sup> In the MD simulations based on the density-functional tight-binding method, it has been suggested that giant fullerenes are first to form from many  $C_2$  clusters and should eventually shrink down to  $C_{60}$ ,  $C_{70}$ , and other larger fullerenes.<sup>24,25</sup> Although these studies have revealed some important aspects of the fullerene formation process, the essential point, the reason why the  $I_h C_{60}$  is special, has not been addressed directly so far.

In the present work, to reveal more details of the microscopic formation process of  $C_{60}$  and other fullerenes, we study the geometries of small carbon clusters and reaction processes between them, mainly using the long-range transferable tight-binding model parametrized by Omata *et al.* (Omata TB).<sup>26</sup> We assume that the fullerene formation originates in many C atoms generated by the vaporization of graphite, on the basis of the two-dimensional NMR experiments of  $^{13}C$ -enriched  $C_{60}$  and  $C_{70}$ ,<sup>27</sup> which have revealed that  $^{13}C$  atoms show neither preferential formation of dimers nor that of larger clusters in the C-C bond network of these fullerenes. Therefore it is natural to expect that the C atoms react with each other to form small carbon clusters in the early stage of the fullerene formation process. Hence we first study the small carbon clusters. We optimize the ground-state geometries of small carbon clusters using the local-density approximation (LDA) in the framework of the density-functional theory (DFT)<sup>28,29</sup> as well as the Omata-TB method. In addition, we study geometries of small carbon clusters at 2000 K using the constant-temperature MD method combined with Omata TB (Omata TBMD). Although fullerenes are formed at the temperature from 1000 to 1500 K in the laser ablation method,<sup>19,30</sup> the MD temperature of the systems is set to be higher than the experimental one so that the small carbon clusters can reach the preferable structure rather promptly within the accessible time period in the TBMD. As a result, it is found that  $C_{10}$  is the smallest stable ring at 2000 K, in good accord with the

high abundance of  $C_{10}$  in the experimental  $C_n^-$  mass spectra.<sup>21,31–34</sup> Considering that the  $C_{10}$  ring should play a role of major constituent units of fullerenes, we next study reactions between two  $C_{10}$  rings with Omata TBMD, and subsequently those between the carbon clusters in which the number of atoms are in multiples of 10, i.e.,  $C_{10m}+C_{10n}$  where  $m$  and  $n$  are natural numbers,  $m+n=2,3,4,5,6$ , and  $m \geq n$ . In addition to these “growth processes,” we consider the possible “shrinkage processes” also using Omata TBMD by studying the structural stabilities of  $C_{50}$ ,  $C_{52}$ ,  $C_{60}$ ,  $C_{62}$ ,  $C_{70}$ , and  $C_{72}$  cages obtained through the reactions between a fullerenelike cage ( $C_{40}$ ) or a fullerene ( $D_{5h} C_{50}$  or  $I_h C_{60}$ ) and a carbon cluster ( $C_{10}$  or  $C_{12}$ ) at various temperatures.

This paper is organized as follows. In Sec. II, the computational methods used in this study, the LDA, Omata TB, and Omata TBMD, are explained. Ground-state geometries and energetics of small carbon clusters and their high-temperature geometries are given in Sec. III. In Sec. IV, the reaction processes between carbon clusters and their products are reported. In Sec. V, the important results in the present study are summarized, and the possible fullerene formation process based on them is discussed. Some remarks are given to conclude this work in Sec. VI.

## II. COMPUTATIONAL METHOD

The DFT<sup>28,29</sup> is known to give highly accurate ground-state geometries and energetics of the various molecules and solids. Furthermore, the first-principles MD method based on the DFT<sup>35</sup> has succeeded in studying various dynamical processes.<sup>36–38</sup> However, the first-principles MD demands much more computer resources than the usual MD methods using interatomic model potential. In particular, in our study of the formation process of fullerenes based on the reactions between carbon clusters, long simulation time should be required. Therefore in the present work, the LDA in the framework of the DFT is only used in the study of ground-state geometries and energetics of small carbon clusters. In the studies of high-temperature geometries of the small carbon clusters and those of the reactions between carbon clusters, we use the constant-temperature MD method combined with the Omata-TB model in order to perform the simulation for a much longer time period than one can perform using the first-principles MD. Omata TBMD requires much less computational efforts than the first-principles MD. Nevertheless, Omata TBMD should give results in good accord with the LDA, as will be discussed in detail in the following.

In the LDA, the Troullier-Martins norm-conserving pseudopotential with Kleinman-Bylander separable approximation is used.<sup>39,40</sup> Wave functions are expanded in terms of the plane-wave basis set with a cutoff energy of 50 Ry. For the exchange-correlation potential, we adopt the parametrized Ceperly-Alder formula.<sup>41,42</sup> Both in the self-consistent electronic-structure calculation and in the geometric-structure optimization the conjugate-gradient procedure is used.<sup>43</sup>

The Omata-TB model, the long-range transferable tight-binding model used in this work, is so parametrized that it can reproduce the energetics of several bulk carbon systems,

such as diamond and graphite, given by the LDA with a well-converged plane wave basis set.<sup>26</sup> The TB model parametrized previously by Xu *et al.*<sup>44</sup> (Xu TB) is known to reproduce well the energetics of the covalent bonds between C atoms. On the other hand, in the model the long-range interatomic interaction cannot be described because the cut-off distance of the interatomic interaction is as short as 2.6 Å, which is much shorter than the interlayer distance of 3.35 Å in “AB” stacking graphite.

Unlike the previous TB model, Omata TB has been so parametrized that it can accurately describe not only the energetics of covalent bonds but also the interlayer interaction between  $sp^2$  layers although the same functional forms as Xu-TB are used. In Omata TB, the cutoff distance of the interatomic interaction is set to be 7.0 Å, which is more or less equal to the maximum reachable distance of the interaction between flat  $sp^2$  layers in the LDA. This elongated cut-off distance enables the model to describe the long-range interatomic forces. In order to discuss the microscopic formation process of fullerenes, this long-range force should play an important role because the long-range force is to be essential for the growth of the  $sp^2$  covalent-bond network in the carbon clusters, as will be shown in Sec. IV.

As the constant-temperature MD method combined with Omata TB, we adopt the Nosé-Hoover MD method<sup>45–47</sup> in order to control the temperature ( $T$ ) of system. In the MD simulation, the shorter the MD time-step length is, the more accurate results should be. Since Omata TB is the method based on electronic-structure calculation, one has to adopt a shorter time step than that for MD simulations with interatomic model potential. Therefore the MD time-step length used in this study is set to be as short as 0.7256 fs.

### III. SMALL CARBON CLUSTERS

In the formation process of fullerenes from C atoms, small carbon clusters should play an important role of the precursor of the fullerenes. Therefore we first study the ground-state geometries and energetics of the  $sp$ -hybridized small carbon clusters using the LDA. We also study them using Omata TB to clarify further the reliability of the Omata TB method. As for the formation process of fullerenes, high-temperature geometries are more essential than the ground-state geometries, since small carbon clusters should be formed at elevated temperature in the formation process of fullerenes. Therefore we next study the high-temperature geometries of small carbon clusters using Omata TBMD.

#### A. Optimized geometry

Previously, the  $sp$ -hybridized small carbon clusters were studied on the basis of the *ab initio* calculations including the effects of polarization functions and electron correlation.<sup>49</sup> In the study, chain and ring forms of the small carbon clusters were optimized within the spin-unrestricted version of the Hartree-Fock approximation (UHF), and ground-state structures were determined by the comparison between binding energies of the two forms calculated by fourth-order Møller-Plesset perturbation theory (MP4). The ground-state geom-

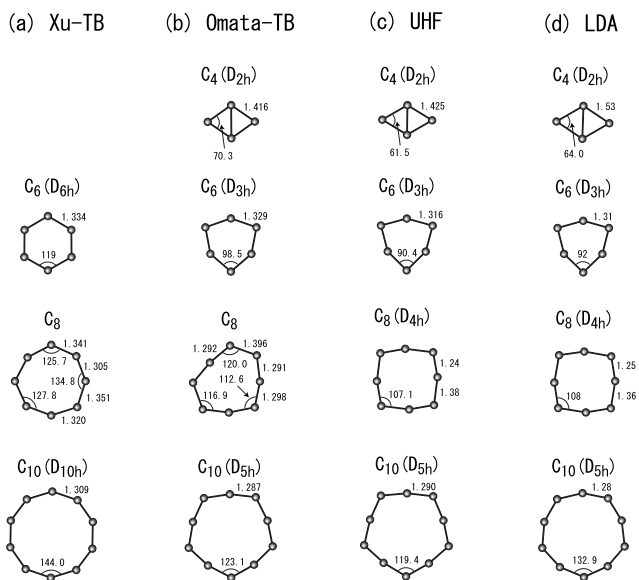


FIG. 1. Geometries of the even-numbered ring clusters,  $C_4$ ,  $C_6$ ,  $C_8$ , and  $C_{10}$ , optimized within (a) Xu TB and (b) Omata TB, respectively, compared with those within (c) the UHF (Ref. 49) and (d) the LDA. The LDA geometry of the  $C_4$  ring is from the literature (Ref. 50). Bond lengths are shown in angstroms and bond angles in degrees. In the case of Xu TB, even though the initial geometry in the optimization procedure of  $C_4$  is set to be a ring,  $C_4$  eventually takes a chain form after the optimization.

etries obtained in this UHF-MP4 theory are found to show the even-odd alternation: the odd-numbered clusters prefer a chain to a ring while the even-numbered clusters prefer a ring to a chain.

In the present work, we optimize chain and ring forms of small carbon clusters within the LDA, Omata TB, and Xu TB, and compare their relative stabilities. Their detailed geometries obtained in each method are compared to those optimized within other methods and to those within the UHF. In particular, we discuss the geometries of the ring clusters in detail, since the ring forms show different geometries depending on their optimization method. The geometries of the even-numbered ring clusters,  $C_4$ ,  $C_6$ ,  $C_8$ , and  $C_{10}$ , optimized within each method are shown in Fig. 1. These four clusters are the only clusters of which geometries can be compared with those optimized within UHF in the literature<sup>49</sup> as well as with those within the LDA.

In the case of the LDA, the  $C_n$  chains ( $3 \leq n \leq 17$ ) and the  $C_n$  rings ( $4 \leq n \leq 24$ ) are studied. In our study, the  $C_2$  and long  $C_n$  chains ( $18 \leq n \leq 24$ ) as well as the  $C_3$  and  $C_4$  rings cannot be optimized due to the ill convergence of the self-consistent calculation. As for the  $C_4$  ring, however, its optimized geometry found in the literature is listed in Fig. 1.<sup>50</sup> As can be seen in Fig. 1, bond angles and symmetries as well as bond lengths of the ring forms of  $C_6$ ,  $C_8$ , and  $C_{10}$ , are in good accord with each other in LDA and in UHF.

Binding energies per atom of the optimized clusters with respect to that of graphene are shown in Fig. 2. In the range of  $8 \leq n \leq 17$ , the binding energy per atom of the  $C_n$  ring is larger than that of the  $C_n$  chain, while that of the  $C_n$  chain is larger than the  $C_n$  ring in  $C_7$  as well as in  $C_5$ . Thus the

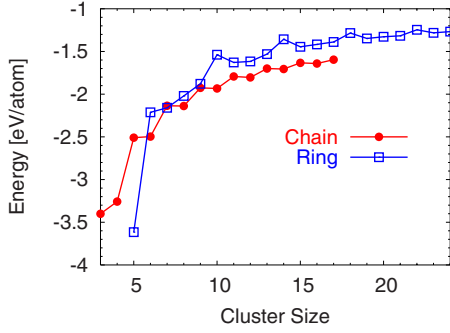


FIG. 2. (Color online) Binding energies per atom of the LDA-optimized  $C_n$  chains ( $3 \leq n \leq 17$ ) and  $C_n$  rings ( $5 \leq n \leq 24$ ) with respect to that of graphene. The binding energy of a  $C_{10}$  ring is larger by 0.4 eV/atom than that of a  $C_{10}$  chain, which is most prominent among the  $C_n$  clusters studied. In the binding energies of  $C_n$  rings, the periodic peaks at  $n=6, 10, 14, 18,$  and  $22$  are observed.

ground-state geometries based on the LDA, unlike the case of UHF-MP4, do not show the even-odd alternation. The binding energy per atom of the  $C_{10}$  ring is 0.4 eV/atom larger than that of the  $C_{10}$  chain. This energetical preference of a ring to a chain in  $C_{10}$  is most prominent among all the  $C_n$  ( $5 \leq n \leq 17$ ) clusters studied. In addition, it is interesting to note that the behavior of the binding energy of the ring form against  $n$  shows the periodic peaks every four atoms at  $n=6, 10, 14, 18,$  and  $22$ . This result may be related to the periodic peaks at  $n=11, 15, 19,$  and  $23$  observed in the  $C_n^+$  mass spectra.<sup>48,49</sup> However, the origin of the one atom difference between the peaks of binding energies of the LDA-optimized rings and those of  $C_n^+$  mass spectra cannot be explained. To clarify this origin, further study is required.

In the case of Omata TB, on the other hand, the  $C_n$  chains ( $3 \leq n \leq 20$ ) and the  $C_n$  rings ( $4 \leq n \leq 20$ ) are optimized. For  $C_3$ , even though the initial geometry of the  $C_3$  ring in the optimization procedure is a ring, the geometry of  $C_3$  transforms into a chain after the optimization. As can be seen from Fig. 1, the bond angles and symmetries as well as bond lengths of the  $C_6$  and  $C_{10}$  rings optimized within Omata TB are in good agreement not only with those optimized within the LDA but also with those within UHF, while the geometry of  $C_8$  optimized within Omata TB is partly different from that within the LDA and that within the UHF. In the geometries optimized within the Xu-TB model, however, their bond angles and symmetries are not in total accord with those obtained by the LDA and UHF, while their bond lengths show good agreement. Further, the comparison between the binding energies of the  $C_n$  ( $3 \leq n \leq 17$ ) chains optimized in the LDA and those in Omata TB with respect to that of graphene is given in Fig. 3, showing that Omata TB can accurately reproduce the energetics of the LDA-optimized chain. Thus Omata TB should give the accurate geometries and energetics of small carbon clusters although the model was constructed so that it can reproduce various bulk geometries and energetics.

### B. Geometry at elevated temperature

Considering that the experimental temperature of fullerene formation in the laser ablation method is

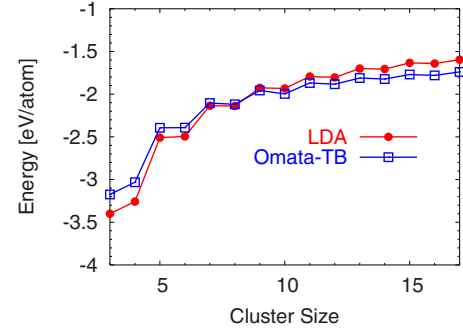


FIG. 3. (Color online) Binding energies per atom of  $C_n$  chains ( $3 \leq n \leq 17$ ) optimized within the LDA and those within Omata TB with respect to that of graphene. Binding energies in Omata TB show good accord with those in the LDA.

1000 to 1500 K,<sup>19,30</sup> small carbon clusters should also be formed at around the same temperature. Therefore high-temperature geometries of small carbon clusters are more important than their ground-state geometries in studying the microscopic formation process of fullerenes. To reveal their high-temperature geometries, we perform the Omata-TBMD simulations of small carbon clusters at  $T=2000$  K, which is set to be higher than the experimental temperature so that the small carbon clusters can promptly reach the high-temperature geometry if it is different from the ground-state geometry. For each small carbon cluster, we adopt the two initial geometries, a chain and a ring optimized within Omata TB. The time length of each simulation is 7.25 ns, corresponding to  $1 \times 10^7$  MD steps. The initial  $1 \times 10^4$  MD steps are used to increase the temperature of system from 1 to 2000 K, and the system is kept at 2000 K for the rest of the period.

For the quantitative discussion of the geometries of clusters at  $T=2000$  K, the indicator to judge whether the geometry of the  $C_n$  cluster at a given MD step is a chain or a ring,  $R$ , is defined as follows:

$$R = \prod_{i=1}^n (\bar{N}_i - 1), \quad (1)$$

$$\bar{N}_i = \begin{cases} 1 & (N_i = 1) \\ 2 & (N_i \geq 2) \end{cases}, \quad (2)$$

where  $N_i$  is the number of atoms surrounding the  $i$ th atom and is defined as the number of atoms within the radius of  $1.8 \text{ \AA}$  from the  $i$ th atom. First, one counts the  $N_i$  of each C atom of the cluster every  $1 \times 10^3$  MD steps. If all the  $N_i$  ( $i = 1, \dots, n$ ) are 2 or larger,  $R=1$ . If, on the other hand, one of  $n$  atoms has only one neighbor like the edge atom of the chain,  $R=0$ . Therefore  $R=0$  corresponds to a chain, and  $R=1$  to a ring. Subsequently, one estimates the time-average value  $\langle R \rangle$  of  $R$  values calculated every  $1 \times 10^3$  MD steps, over  $1 \times 10^5$  to  $1 \times 10^7$  MD steps. In order to exclude the initial-geometry dependence as much as possible and to observe the average geometries at  $T=2000$  K, the  $R$  values of the initial  $1 \times 10^5$  MD steps are not included in the calcula-

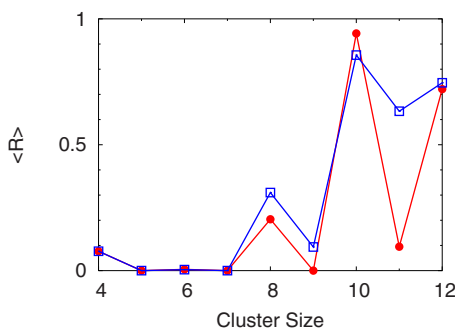


FIG. 4. (Color online)  $\langle R \rangle$  values of each small carbon cluster at 2000 K with two initial geometries, a chain and a ring. Circles represent  $\langle R \rangle$  in the case where the initial geometry is a chain, and squares in the case where it is a ring. Here,  $R$  is the indicator, defined as formulas (1) and (2), to judge whether the geometry of the cluster at the MD step is a chain or a ring;  $R=0$  corresponds to a chain, and  $R=1$  to a ring. The  $\langle R \rangle$  is the time average of  $R$  calculated every  $1 \times 10^3$  MD steps over  $1 \times 10^5 - 1 \times 10^7$  MD steps.

tion of  $\langle R \rangle$ . From the definition of  $R$  therefore clusters with  $\langle R \rangle$  close to 1 prefer a ring to a chain while those with  $\langle R \rangle$  close to 0 prefer a chain to a ring.

In Fig. 4, two  $\langle R \rangle$  values of each small carbon cluster are given, corresponding to two initial geometries, a chain and a ring. In the clusters except for  $C_{11}$ , the  $\langle R \rangle$  values show the weak dependence on the initial geometries. The  $\langle R \rangle$  values of the clusters,  $C_5$ ,  $C_6$ ,  $C_7$ , and  $C_9$ , nearly equal to 0, show the strong preference of a chain to a ring. Also,  $C_4$  and  $C_8$  prefer a chain to a ring because the two  $\langle R \rangle$  values of  $C_4$  are 0.08 regardless of initial geometries, and those of  $C_8$  are 0.20 and 0.31. From these results, in the range of  $4 \leq n \leq 9$ , the free energies of a  $C_n$  chain are expected to be lower than that of a  $C_n$  ring at 2000 K, although the binding energies of ring forms are larger than those of chain forms in  $C_6$  and  $C_8$  (Fig. 2). On the other hand,  $C_{10}$  and  $C_{12}$  prefer a ring to a chain because the two  $\langle R \rangle$  values of  $C_{10}$  are 0.86 and 0.94, and those of  $C_{12}$  are 0.72 and 0.75. Interestingly, the  $\langle R \rangle$  values of  $C_{10}$  is closest to 1 in the carbon clusters studied, indicating the remarkable stability of the  $C_{10}$  ring. Exceptionally,  $C_{11}$  shows the different  $\langle R \rangle$  values depending on the initial geometry;  $\langle R \rangle=0.10$  in the case where the initial geometry is a chain while  $\langle R \rangle=0.63$  in the case where it is a ring. In the case where the initial geometry is a chain, a chain is isomerized into a ring at  $9 \times 10^6$  MD steps, and the ring form is kept for the rest of the period. Therefore it is expected that the longer-period time simulation will increase the  $\langle R \rangle$  value even in the case where the initial geometry is a chain, and eventually  $C_{11}$  would prefer a ring to a chain regardless of initial geometries.

Among these results, it should be most important that  $C_{10}$  is the smallest stable ring at 2000 K. This result is considered to reflect the prominent energetical preference of a ring to a chain in the LDA-optimized  $C_{10}$  (Fig. 2). In addition, the free energy of a  $C_{10}$  ring should be much lower than that of a  $C_{10}$  chain at 2000 K. Under the circumstances where small carbon clusters are formed, rings are expected to survive more prominently than chains, since chains should have the

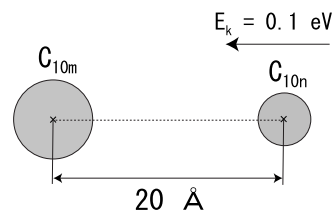


FIG. 5. Schematic picture of the initial condition in the reactions of  $C_{10m} + C_{10n}$  where  $m$  and  $n$  are natural numbers,  $m+n=2, 3, 4, 5, 6$ , and  $m \geq n$ . The distance between their gravity centers of the  $C_{10m}$  and  $C_{10n}$  is set to be  $20 \text{ \AA}$ . The  $C_{10n}$  has the barycentric velocity corresponding to the kinetic energy of 0.1 eV toward the gravity center of the  $C_{10m}$ .

higher reactivity than rings due to their edge atoms possessing a dangling bond. Therefore this remarkable stability of the  $C_{10}$  ring at elevated temperature is considered to be responsible for the high abundance of  $C_{10}$  in the experimental  $C_n^-$  mass spectra.<sup>21,31-34</sup>

#### IV. REACTION BETWEEN CARBON CLUSTERS

From the result that  $C_{10}$  is the smallest stable ring at  $T=2000$  K obtained in the preceding section as well as from the high abundance of  $C_{10}$  in the experimental  $C_n^-$  mass spectra, it is expected that  $C_{10}$  rings are formed in abundance at the initial stage of the formation process of fullerenes as well. Therefore considering that the  $C_{10}$  ring should play a role of major constituent units of fullerenes, we study the reaction between two  $C_{10}$  rings, and then those between carbon clusters possessing the number of C atoms in multiples of 10,  $C_{10m} + C_{10n}$  where  $m$  and  $n$  are natural numbers,  $m+n=2, 3, 4, 5, 6$ , and  $m \geq n$ , with Omata TBMD. Initial conditions in all the cases are given in Fig. 5. At the initial time, the  $C_{10m}$  and  $C_{10n}$  clusters have the geometries obtained by the Omata-TBMD simulation at the same temperature, and the distance between their gravity centers of the two clusters is set to be  $20 \text{ \AA}$ . In addition, the  $C_{10n}$  has the barycentric velocity corresponding to the kinetic energy ( $E_k$ ) of 0.1 eV toward the gravity center of the  $C_{10m}$  having no barycentric velocity so that the two clusters collide with each other. These simulations of the reactions of  $C_{10m} + C_{10n}$  are performed for the period of 7.25 ns, corresponding to  $1 \times 10^6$  MD steps.

##### A. $C_{10} + C_{10}$

Under the circumstances where the  $C_{10}$  ring is abundant, reaction events among  $C_{10}$  rings should occur at a high rate. For the discussion of the formation process of fullerenes from  $C_{10}$  rings, the study of the reaction process between two  $C_{10}$  rings ( $C_{10} + C_{10}$ ) is important. Therefore we first study the reaction of  $C_{10} + C_{10}$  at  $T=1000, 1500, 2000$ , and  $2500$  K. At the temperature of 1000–2000 K, the two  $C_{10}$  rings coalesce into a  $sp^2$ -hybridized  $C_{20}$  plane. The detailed reaction process at  $T=1500$  K, in which the growth of the  $sp^2$  network is found to be more prominent than in the case of  $T=1000$  K and the reaction process is slower and there-

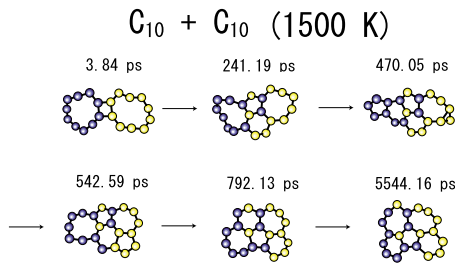


FIG. 6. (Color online) Snapshots of the reaction process of  $C_{10}+C_{10}$  in the case of  $T=1500$  K with Omata TBMD. Two  $C_{10}$  rings collide with each other, and then coalesce into the  $sp^2$ -hybridized  $C_{20}$  plane. Blue (dark gray) and yellow (light gray) spheres represent the atoms which initially formed two different  $C_{10}$  rings, respectively. It is interesting to note that the C atoms of the originally different  $C_{10}$  rings are already mixed in the final  $C_{20}$  plane.

fore more traceable than in the case of  $T=2000$  K, is given in Fig. 6. The geometry of the  $C_{20}$  plane at 792.13 ps consists of a pentagon, two hexagons, and two heptagons. At 5544.16 ps, a hexagon and a heptagon in the  $C_{20}$  plane exchange their positions. Interestingly, it is observed that C atoms which initially formed two different  $C_{10}$  rings are already mixed in the  $C_{20}$  plane, which indicates that the plane geometry of  $C_{20}$  obtained would be more or less independent of the detailed geometry of the initial  $C_{10}$  rings. At higher temperature,  $T=2500$  K,  $C_{20}$  is initially formed, and then the  $C_{20}$  decays into  $C_{17}$  via  $C_3$  loss process at 4031.72 ps, and further into  $C_{15}$  via  $C_2$  loss process at 5032.76 ps.

We also study the reaction of  $C_{10}+C_{10}$  using the MD method combined with Xu TB (Xu TBMD). In this case, two  $C_{10}$  rings do not coalesce after their collision, but bounce each other at all the temperatures. Thus Omata TBMD and Xu TBMD give different results. The growth of the  $sp^2$  network can be seen in the case of Omata TBMD while it cannot be seen in the case of Xu TBMD. This difference should be attributed to the long-range interaction incorporated in the Omata TB as mentioned earlier. In the formation process of fullerenes, the precursor carbon clusters should have the  $sp^2$ -network structure because the fullerene structure would be more easily formed from the  $sp^2$ -network geometries than directly from  $sp$  geometries. Therefore the long-range interactions are of essential importance in studying the microscopic formation process of fullerenes.

### B. Formation of $C_{30}$ , $C_{40}$ , $C_{50}$ , and $C_{60}$

The study of the reaction of  $C_{10}+C_{10}$  has revealed that the  $sp^2$ -hybridized  $C_{20}$  plane can be formed from  $C_{10}$  rings. Subsequently, it is expected that the  $C_{20}$  cluster reacts with  $C_{10}$  or other  $C_{20}$  clusters, and eventually grows into  $C_{30}$  or  $C_{40}$  clusters. Therefore we next study the reactions of  $C_{20}+C_{10}$  and  $C_{20}+C_{20}$  at  $T=1000$ , 1500, 2000, and 2500 K. In both cases, the initial geometry of  $C_{20}$  is that at 362.70 ps in the reaction of  $C_{10}+C_{10}$ . As has been mentioned in the previous subsection, in the reaction process of  $C_{10}+C_{10}$  at 2500 K, the product,  $C_{20}$ , is later subject to sequential  $C_3$  and  $C_2$  losses at 4031.72 and 5032.76 ps, respectively.

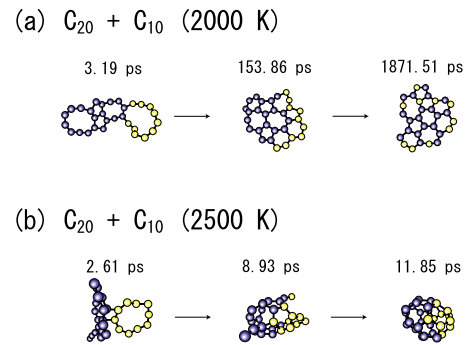


FIG. 7. (Color online) Snapshots of the reaction processes of  $C_{20}+C_{10}$  at (a)  $T=2000$  K and (b) 2500 K. Blue (dark gray) and yellow (light gray) spheres represent the atoms of the initial  $C_{20}$  plane, and those of the initial  $C_{10}$  ring, respectively. In the reaction (a), the  $sp^2$ -hybridized  $C_{30}$  plane mainly consisting of pentagons and hexagons is formed, and the C atoms of the initial  $C_{10}$  ring are distributed over the entire  $C_{30}$  cluster. In the reaction (b), the  $sp^2$ -hybridized fullerene-like  $C_{30}$  closed cage is formed.

The reaction of  $C_{20}+C_{10}$  gives three different results, depending on the temperature of the system. At  $T=1000$  K, the  $C_{30}$  cluster possessing an  $sp^2$ -plane part as well as  $sp$ -ring parts. At  $T=1500$  and 2000 K, on the other hand, the  $sp^2$ -hybridized  $C_{30}$  plane consisting mainly of pentagons and hexagons is formed, as shown in Fig. 7(a). In the final geometry of the  $C_{30}$  plane, ten C atoms of the initial  $C_{10}$  ring are found to be distributed over the entire cluster. At  $T=2500$  K, an  $sp^2$ -hybridized fullerene-like  $C_{30}$  closed cage is formed, as can be seen in Fig. 7(b).

The reaction of  $C_{20}+C_{20}$  also shows three different results, depending on the differences of the temperatures. At  $T=1000$  and 1500 K, an  $sp^2$ -hybridized  $C_{40}$  plane is formed. At  $T=2000$  K, as can be seen in Fig. 8(a), the  $C_{40}$  plane is initially formed, and then transforms into a basketlike form, and finally gives rise to a fullerene-like  $C_{40}$  cage. The resulting  $C_{40}$  cage is much more compact than the initial  $C_{40}$  plane, which implies that the isomerization of the

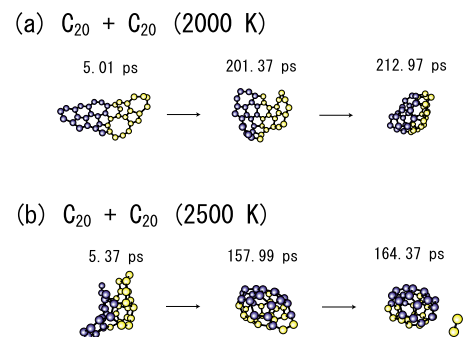


FIG. 8. (Color online) Snapshots of the reaction processes of  $C_{20}+C_{20}$  at (a)  $T=2000$  K and (b) 2500 K. Blue (dark gray) and yellow (light gray) spheres represent the atoms which initially formed two different  $C_{20}$  planes, respectively. In the reaction (a), the  $sp^2$ -hybridized fullerene-like  $C_{40}$  closed cage is formed. In the reaction (b), the fullerene-like  $C_{40}$  cage is formed, and then the  $C_{40}$  cage decays into  $C_{38}$  cage through  $C_2$  loss.

TABLE I. Final geometries obtained through the reactions of  $C_{10m}+C_{10n}$  ( $m+n=2,3,4,5,6, m \geq n$ ).

Reaction	1500 K	2000 K	2500 K
$C_{10}+C_{10}$	plane $C_{20}$	plane $C_{20}$	$C_{15}+C_3+C_2$
$C_{20}+C_{10}$	plane $C_{30}$	plane $C_{30}$	cage $C_{30}$
$C_{20}+C_{20}$	plane $C_{40}$	cage $C_{40}$	cage $C_{38}+C_2$
$C_{30}+C_{10}$	cage $C_{40}$	plane $C_{40}$	cage $C_{40}$
$C_{30}+C_{20}$	cage $C_{50}$	cage $C_{50}$	cage $C_{50}$
$C_{40}+C_{10}$	cage $C_{50}$	cage $C_{50}$	cage $C_{50}$
$C_{30}+C_{30}$	cage $C_{60}$	cage $C_{60}$	cage $C_{60}$
$C_{40}+C_{20}$	cage $C_{60}$	cage $C_{60}$	cage $C_{60}$
$C_{50}+C_{10}$	cage $C_{60}$	cage $C_{60}$	cage $C_{60}$

$sp^2$ -hybridized plane into a fullerenelike cage leads to the reduction of a collision cross section with other clusters. At  $T=2500$  K, the  $C_{40}$  cage is formed, and then decays into a  $C_{38}$  cage through the  $C_2$  loss process, as shown in Fig. 8(b). Through this  $C_2$  loss process, the local strain of the cage structure, observed at 157.99 ps, seems to be relieved, and eventually a pentagon and a hexagon are formed at 164.37 ps. The  $C_2$  loss process of fullerenelike cages will be discussed in detail later.

The  $C_{30}$  and  $C_{40}$ , obtained through the reactions of  $C_{20}+C_{10}$  and  $C_{20}+C_{20}$ , should grow into larger clusters, such as  $C_{40}$ ,  $C_{50}$ ,  $C_{60}$ , and  $C_{70}$ , etc., through reactions with other clusters. Therefore we study six sets of reactions of  $C_{30}+C_{10}$ ,  $C_{30}+C_{20}$ ,  $C_{40}+C_{10}$ ,  $C_{30}+C_{30}$ ,  $C_{40}+C_{20}$ , and  $C_{50}+C_{10}$  at  $T=1500$  K for the formation of  $C_{40}$ ,  $C_{50}$ , and  $C_{60}$ , respectively. In these reactions, the initial geometries of  $C_{20}$ ,  $C_{30}$ , and  $C_{40}$  used are the geometries at 362.70 ps in the previous reactions of  $C_{10}+C_{10}$ ,  $C_{20}+C_{10}$ , and  $C_{20}+C_{20}$ , respectively. As for the initial geometry of  $C_{50}$ , the geometry of the reaction process  $C_{30}+C_{20}$  at 362.70 ps is used. These simulations are also performed at 2000 and 2500 K. However, the initial geometry of the  $C_{40}$  at 2500 K is the geometry at 362.70 ps in the reaction of  $C_{30}+C_{10}$ , since in the reactions of  $C_{20}+C_{20}$  at 2500 K the  $C_{40}$  product has already decayed into  $C_{38}$  at 164.37 ps.

The final geometries obtained through these six sets of reactions as well as the three sets of reactions of  $C_{10}+C_{10}$ ,  $C_{20}+C_{10}$ , and  $C_{20}+C_{20}$  at  $T=1500, 2000,$  and  $2500$  K are summarized in Table I. In most cases,  $C_{20}$  and  $C_{30}$  form the  $sp^2$ -hybridized planes, while  $C_{40}$ ,  $C_{50}$ , and  $C_{60}$  take the  $sp^2$ -hybridized fullerenelike cage geometries. In particular,  $C_{40}$ ,  $C_{50}$ , and  $C_{60}$  cages can be formed as low as 1500 K, which is in good accord with the experimental temperature of fullerene formation, from 1000 to 1500 K.<sup>19,30</sup> The  $C_{40}$ ,  $C_{50}$ , and  $C_{60}$  clusters may have the fullerenelike cage geometry even at temperatures lower than  $T=1500$  K. At 2500 K, even  $C_{30}$  takes the closed-cage geometry. These results are in good accord with the experimental results of the gas ion chromatography where  $C_{30}$  is the smallest fullerenelike closed-cage cluster and the fullerenelike cage structure is most favorable in  $C_{50}$  or larger carbon clusters.<sup>51</sup> In order to determine the smallest closed-cage cluster, one has to study further other-size clusters between  $C_{20}$  and  $C_{30}$  at various temperatures.

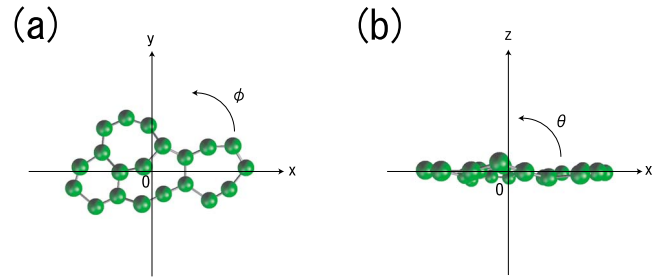


FIG. 9. (Color online) Rotational angles of the initial  $C_{20}$  plane,  $\phi$  and  $\theta$ , are defined as (a) the rotational angle around the  $z$  axis and (b) that around the  $y$  axis, respectively. The gravity center of  $C_{20}$  is at the origin in Cartesian coordinates.

### C. Dependence on collision conditions

Although the  $sp^2$ -hybridized planes and fullerenelike cages have been obtained through the reactions of  $C_{10m}+C_{10n}$ , these final geometries may depend on specific collision conditions. Therefore we study the reactions of  $C_{20}+C_{10}$  and  $C_{20}+C_{20}$  at  $T=2000$  K with several different collision conditions, and then check the dependence of the final geometries on the collision conditions. In both cases, the initial geometry of  $C_{20}$  is the  $sp^2$  plane, obtained at 362.70 ps in the reaction of  $C_{10}+C_{10}$  at  $T=2000$  K, and the initial  $C_{10}$  ring also has the geometry obtained by the Omata-TBMD simulations at  $T=2000$  K. Different collision conditions are generated by rotating one initial  $C_{20}$  plane without rotating the  $C_{10}$  ring or the other  $C_{20}$  plane. The  $C_{20}$  plane to be rotated is put on the  $x$ - $y$  plane in Cartesian coordinates with the gravity center of the  $C_{20}$  at the origin in Cartesian coordinates. For the rotation of the  $C_{20}$  plane,  $\phi$  and  $\theta$  are defined as the rotational angle around the  $z$  axis and that around the  $y$  axis, respectively, as shown in Fig. 9. As many as nine sets of  $\phi$  and  $\theta$ ,  $(\phi, \theta)=(0, 0), (0, 15), (0, 30), (0, 45), (0, 60), (0, 75), (0, 90), (45, 0),$  and  $(90, 0)$  in degrees, are considered for both reactions of  $C_{20}+C_{10}$  and  $C_{20}+C_{20}$ , respectively. On the other hand, the  $C_{10}$  ring in the reaction of  $C_{20}+C_{10}$  and the other  $C_{20}$  plane in the reaction of  $C_{20}+C_{20}$  are put on the  $x$ - $y$  plane, and they are not rotated.

The reactions of  $C_{20}+C_{10}$  are found to generate the planar  $C_{30}$  as a final geometry in most  $(\phi, \theta)$  cases. Only in the case of  $(\phi, \theta)=(0, 90)$  is a  $C_{30}$  cage formed. On the contrary, the reactions of  $C_{20}+C_{20}$  end up with a  $C_{40}$  cage in most  $(\phi, \theta)$  cases. Only in the case of  $(\phi, \theta)=(0, 60)$  is a planar  $C_{40}$  formed. Thus regardless of the collision conditions, it is confirmed that a  $C_{30}$  plane and a  $C_{40}$  cage are naturally formed at around  $T=2000$  K. This confirms the relatively weak dependence of the reaction products on the details of the initial conditions. Therefore most of the other reactions of  $C_{10m}+C_{10n}$  in the previous subsection also should give the similar final geometries even under the different initial conditions.

### D. $C_2$ loss of fullerenelike cages

The study of the reactions of  $C_{10m}+C_{10n}$  has shown the straightforward growth of a network structure of carbon clusters: from an  $sp$ -hybridized ring to an  $sp^2$ -hybridized plane,

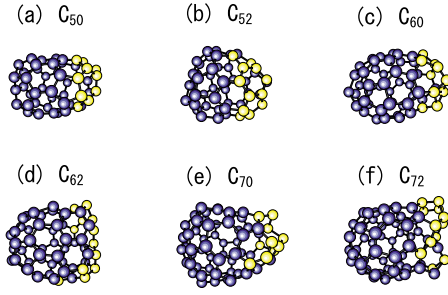


FIG. 10. (Color online) Geometries of rather spherical fullerene-like (a)  $C_{50}$ , (b)  $C_{52}$ , (c)  $C_{60}$ , (d)  $C_{62}$ , (e)  $C_{70}$ , and (f)  $C_{72}$  cages to shrink through the  $C_2$  loss process, which are obtained through the reactions of  $C_{40}+C_{10}$  at 1095.34 ps ( $T=2460$  K),  $C_{40}+C_{12}$  at 211.81 ps ( $T=2500$  K),  $C_{50}(D_{5h})+C_{10}$  at 362.70 ps ( $T=2510$  K),  $C_{50}(D_{5h})+C_{12}$  at 109.53 ps ( $T=2480$  K),  $C_{60}(I_h)+C_{10}$  at 362.70 ps ( $T=2425$  K), and  $C_{60}(I_h)+C_{12}$  at 72.54 ps ( $T=2420$  K), respectively. Blue (dark gray) and yellow (light gray) spheres represent the atoms of the original  $C_{40}$ ,  $C_{50}$ , or  $C_{60}$  cage and those of the  $C_{10}$  or  $C_{12}$ , respectively.

and from an  $sp^2$ -hybridized plane to a fullerene-like cage. Only through the growth process, however, fullerenes larger than  $C_{60}$  should be more abundant, since the larger fullerenes, such as  $C_{70}$  and  $C_{84}$ , are energetically more stable than  $C_{60}$ .<sup>12,13</sup> Therefore the shrinkage process of fullerenes larger than  $C_{60}$  as well as the growth process must be essential for the remarkable high abundance of  $C_{60}$ .

In order to discuss the shrinkage process of fullerenes, we study the structural stabilities of fullerene-like  $C_{50}$ ,  $C_{52}$ ,  $C_{60}$ ,  $C_{62}$ ,  $C_{70}$ , and  $C_{72}$  cages obtained through the reactions between a fullerene-like cage ( $C_{40}$ ) or a fullerene ( $D_{5h}$   $C_{50}$  or  $I_h$   $C_{60}$ ) and a small carbon cluster ( $C_{10}$  or  $C_{12}$ ), at the temperatures of  $T_k=2400+5k$  [K] ( $k=0, 1, \dots, 40$ ). Initial conditions are given as follows. The distance between the fullerene-like cage or fullerene and the small carbon cluster is set to be 15 Å. The initial fullerene-like cage or fullerene and small carbon cluster have the geometries obtained through the Omata-TBMD simulation at the temperature of  $T_k$ . In addition, the small carbon cluster has the barycentric velocity corresponding to the kinetic energy of 0.1 eV toward the gravity center of the fullerene-like cage or fullerene having no barycentric velocity so that the small carbon cluster shall collide with the fullerene-like cage or fullerene. The time length of each simulation is 2.90 ns, corresponding to  $4 \times 10^6$  MD steps.

In some cases, it is found that the  $C_{50}$ ,  $C_{52}$ ,  $C_{60}$ ,  $C_{62}$ ,  $C_{70}$ , and  $C_{72}$  cages shrink into  $C_{48}$ ,  $C_{50}$ ,  $C_{58}$ ,  $C_{60}$ ,  $C_{68}$ , and  $C_{70}$  cages through  $C_2$  loss, respectively. It is found that even “spherical” cages sometimes show  $C_2$  loss eventually in the MD simulation. Typical geometries of “spherical”  $C_{50}$ ,  $C_{52}$ ,  $C_{60}$ ,  $C_{62}$ ,  $C_{70}$ , and  $C_{72}$  to shrink through the  $C_2$  loss process are shown in Fig. 10. The  $C_2$  loss is known to be observed in the experiment of the laser-induced fragmentation of carbon clusters.<sup>52</sup> In these cases as well as in the reactions of  $C_{20}+C_{20}$  at 2500 K, the  $C_2$  loss process of cages occurs at their area where structural strain seems to concentrate locally. In this study, the loss of  $C_3$  or larger units of the cages is not observed. Hence the  $C_2$  loss should be the most important

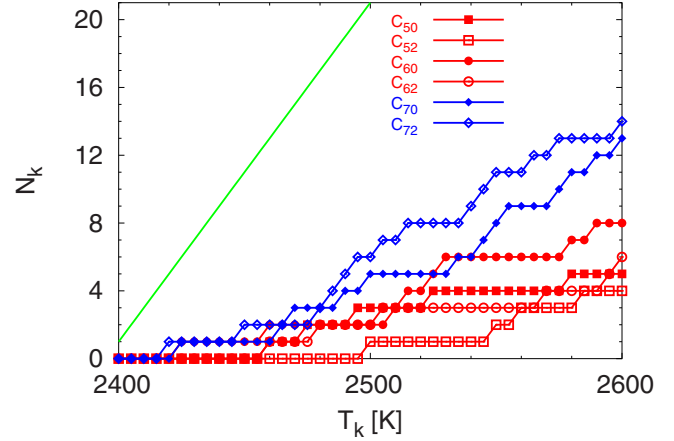


FIG. 11. (Color online)  $N_k$  values ( $k=0, 1, 2, \dots, 40$ ) of fullerene-like  $C_{50}$ ,  $C_{52}$ ,  $C_{60}$ ,  $C_{62}$ ,  $C_{70}$ , and  $C_{72}$  cages, defined by formula (3), as a function of  $T_k$ . The straight line represents the case where  $C_2$  loss occurs at all the temperatures. In the behavior of  $N_k$ , only a small difference among  $C_{50}$ ,  $C_{52}$ ,  $C_{60}$ , and  $C_{62}$  can be seen. However,  $N_k$  values of  $C_{70}$  and  $C_{72}$  increase much more rapidly than those of other cages as a function of temperature.

process for carbon clusters larger than  $C_{60}$  to shrink in the formation process of fullerenes.

Therefore we study the rates of  $C_2$  loss of the  $C_{50}$ ,  $C_{52}$ ,  $C_{60}$ ,  $C_{62}$ ,  $C_{70}$ , and  $C_{72}$  cages, and compare their relative  $C_2$  loss rates through the value  $N_k$  ( $k=0, 1, \dots, 40$ ), defined by the following formula:

$$N_k = \sum_{i=0}^k D(T_i), \quad (3)$$

where  $D(T_k)$  is defined as the indicator of the occurrence of  $C_2$  loss. If  $C_2$  loss occurs at  $T_k$  [K] during the entire simulation time of 2.90 ns,  $D(T_k)=1$ , while  $D(T_k)=0$  otherwise. Results are shown in Fig. 11. It is rather evident that those clusters form two groups; four clusters of  $C_{50}$ ,  $C_{52}$ ,  $C_{60}$ , and  $C_{62}$ , and the remaining two clusters  $C_{70}$  and  $C_{72}$ .  $N_k$  values of  $C_{70}$  and  $C_{72}$  rise much steeper than those of the other cages as a function of the temperature. The  $C_2$  loss rates of  $C_{70}$  and  $C_{72}$  are much larger than those of other cages. Therefore it is expected that fullerene-like cages larger than  $C_{60}$  shrink through  $C_2$  loss at a higher rate.

In addition, to reveal the temperature at which symmetrical fullerenes shrink through  $C_2$ , we also study those of  $D_{5h}$   $C_{50}$ ,  $I_h$   $C_{60}$ , and  $D_{5h}$   $C_{70}$  fullerenes at the temperatures of  $T_k=2000+50k$  [K] ( $k=0, 1, \dots, 30$ ). These simulations are performed for the same time length as that in the case of fullerene-like cages. In the cases of  $C_{50}$  and  $C_{70}$ ,  $C_2$  loss occurs at  $3050 \leq T_k \leq 3500$  [K]. In the case of  $C_{60}$ ,  $C_2$  loss occurs at  $T_k=3000$  K and  $3100 \leq T_k \leq 3500$  [K]. Thus these fullerenes shrink through  $C_2$  loss at more than around  $T_k=3000$  K. It is much higher than the temperature at which the fullerene-like cages studied shrink through  $C_2$  loss. Strain would be less likely to concentrate at a local area in these fullerenes than in fullerene-like cages, giving rise to their higher stability against the  $C_2$  loss.

## V. DISCUSSION

In the present work, we have obtained several important results which should be the keys to elucidate the mystery of the formation process of fullerenes. First, the study of the small carbon clusters reveals the remarkable stability of the  $C_{10}$  ring. From the LDA geometry-optimization study, it is found that the binding energy per atom of the  $C_{10}$  ring is by 0.4 eV/atom larger than that of the  $C_{10}$  chain, which is most prominent among all  $C_n$  clusters studied ( $5 \leq n \leq 17$ ). More importantly, the Omata-TBMD study has confirmed that  $C_{10}$  is the smallest stable ring at  $T=2000$  K. These results explain the high abundance of  $C_{10}$  in the experimental  $C_n^-$  mass spectra.<sup>21,31-34</sup> Therefore the  $sp$ -hybridized  $C_{10}$  ring should play an important role in the formation process of fullerenes.

Second, it is confirmed that  $sp^2$ -hybridized planes and fullerene-like cages are obtained through reaction between two  $C_{10}$  rings and those between the carbon clusters possessing the C atoms in multiples of 10,  $C_{10m}+C_{10n}$  where  $m$  and  $n$  are natural numbers,  $m+n=2,3,4,5,6$ , and  $m \geq n$ , at several temperatures. In the Omata-TBMD simulation, unlike the case of the MD method combined with the previous TB model, the reaction of  $C_{10}+C_{10}$  gives rise to the  $sp^2$ -hybridized  $C_{20}$  plane, which indicates the high importance of long-range interatomic force. In most cases studied,  $C_{20}$  and  $C_{30}$  have the  $sp^2$ -hybridized plane while  $C_{40}$ ,  $C_{50}$ , and  $C_{60}$  take the  $sp^2$ -hybridized fullerene-like cage geometries. In particular,  $C_{40}$ ,  $C_{50}$ , and  $C_{60}$  cages can be formed at temperatures as low as 1500 K, which is in good agreement with the experimental temperature of fullerene formation, from 1000 to 1500 K.<sup>19,30</sup> In a few cases, even  $C_{30}$  has the cage structure. These results are in good accord with the experimental results of the gas ion chromatography.<sup>51</sup> Considering that the final geometries in the reactions of  $C_{20}+C_{10}$  and  $C_{20}+C_{20}$  have the weak dependence on the collision conditions, the other reactions of  $C_{10m}+C_{10n}$  also should give similar results even under different initial conditions. The straightforward growth process from the  $sp$ -hybridized ring to the  $sp^2$ -hybridized plane, and that from the  $sp^2$ -hybridized plane to the  $sp^2$ -hybridized fullerene-like cage should be essential for the formation of fullerenes.

Last, the study of structural stabilities of cage geometries obtained through the reactions between a fullerene-like cage ( $C_{40}$ ) or a fullerene ( $D_{5h} C_{50}$  or  $I_h C_{60}$ ) and a small carbon cluster ( $C_{10}$  or  $C_{12}$ ) at various temperatures with Omata TBMD indicates the possibility that fullerenes larger than  $C_{60}$  tend to shrink through the  $C_2$  loss process at a higher rate. It is confirmed that the  $C_2$  loss rates of the  $C_{70}$  and  $C_{72}$  cages are much higher than those of the  $C_{50}$ ,  $C_{52}$ ,  $C_{60}$ , and  $C_{62}$  cages. From these results, it is expected that fullerene-like cages larger than  $C_{60}$  shrink through  $C_2$  loss at a higher rate than  $C_{60}$  or smaller fullerene-like cages.

From the above-mentioned results obtained through the present work as well as from the high abundance of  $C_{10}$ , we propose the following formation process of fullerenes. Initially, many C atoms are generated through the vaporization of graphite. Subsequently, the C atoms collide with each other, and then  $C_{10}$  rings are formed in abundance. These  $C_{10}$  rings must react with each other, and  $C_{10n}$  ( $n=2,3,\dots$ ), clus-

ters should become abundant clusters in the next stage. These  $C_{10n}$  clusters are to have  $sp^2$ -hybridized plane or fullerene-like closed-cage geometries, according to the present results that a  $C_{30}$  or larger cluster can have the fullerene-like cage geometry. The larger the clusters are, the more easily they form fullerene-like cages. The probability that a fullerene-like cage collides with other clusters should be lower than that of a planar cluster due to its smaller collision cross section. At elevated temperature, the fullerene-like cages are isomerized into symmetrical fullerenes consisting only of pentagons and hexagons, through the migration of their C atoms. If, however, the growth process is the only process during the fullerene formation, the fullerenes larger than  $C_{60}$ , which are energetically more stable than  $C_{60}$ , should be more abundant. Therefore the process to prevent the formation of fullerenes larger than  $C_{60}$  as well as the growth process through reactions among carbon clusters is essential for the remarkable high abundance of  $C_{60}$ . We consider that the main factor to prevent the formation of fullerenes larger than  $C_{60}$  is the shrinkage process of fullerene-like cages through  $C_2$  loss. If our observation that fullerene-like cages larger than  $C_{60}$  decay through  $C_2$  loss at a higher rate than  $C_{60}$  or smaller fullerene-like cages is the universal tendency in even larger fullerene-like cages, it is expected that these cages shrink into smaller ones through the sequential  $C_2$  losses, and eventually  $C_{60}$  becomes the most abundant fullerene. Through the same process, other abundant fullerenes, such as  $C_{70}$  and  $C_{84}$ , are expected to be formed. Thus we consider that the competition between the growth process through the reactions among  $C_{10n}$  ( $n=1,2,\dots$ ) clusters and the shrinkage process of fullerene-like cages through  $C_2$  loss determines the relative abundance of fullerenes, leading to the remarkable high abundance of  $C_{60}$ .

In addition, very low reactivity of  $I_h C_{60}$  also should contribute to the high abundance of  $C_{60}$ . The fullerenes smaller than  $C_{70}$ , except for  $C_{60}$ , do not satisfy the IPR. These IPR-breaking fullerenes are unextractable from carbon soot. In the structures of the IPR-breaking fullerenes, there are atoms shared by adjacent pentagons, which should possess not  $sp^2$ -like but  $sp^3$ -like hybridization character.<sup>15</sup> Therefore the IPR-breaking fullerenes must be much more reactive than the IPR-satisfying ones. The more reactive a fullerene is, the more easily the fullerene will grow into larger fullerenes through the reaction with other clusters. Hence the IPR should indicate the high importance of the reactivities in the formation process of fullerenes. Actually, our previous density-functional study<sup>16</sup> has quantitatively confirmed that the IPR-breaking fullerene  $C_{50}$  is much more reactive than the IPR-satisfying fullerenes  $C_{60}$  and  $C_{70}$ . More importantly, it has been revealed that  $C_{70}$  is more reactive than  $C_{60}$ . Therefore it is expected that  $C_{70}$  reacts with other clusters more easily than  $C_{60}$ . This must enhance the high abundance of  $C_{60}$  compared with  $C_{70}$ . Thus once  $I_h C_{60}$  is formed through the competition between the growth process and shrinkage process, the  $C_{60}$  is least likely to grow further due to its low reactivity among the IPR-satisfying fullerenes.

## VI. CONCLUDING REMARKS

Through the present work, we have confirmed the remarkable stability of the  $C_{10}$  ring. Therefore in the formation pro-

cess of fullerenes the  $C_{10}$  ring should play a role of major constituent units of fullerenes. On the basis of the present results obtained through the molecular-dynamics study combined with the transferable tight-binding model with long-range interaction properly taken into account, we propose the formation process of fullerenes where the competition between the growth process through the reactions among  $C_{10n}$  ( $n=1, 2, \dots$ ) clusters and the shrinkage process through  $C_2$  loss determines the relative abundance of fullerenes, leading to the remarkable high abundance of  $C_{60}$ . In the growth process, reactions among the  $C_{10n}$  clusters would give rise to the  $sp^2$ -hybridized plane or the fullerene-like cage. Their formation process requires neither specific collision conditions nor the sequence of collisions among the  $C_{10n}$  clusters. In the shrinkage process, the  $C_2$  loss process of fullerene-like cages, instead of  $C_3$  or larger units, is to be the most important process. Since the  $C_{10}$  cluster reaction is of high importance, this formation process may be called the “ $C_{10}$  reaction road.” Obviously, in order to confirm the reliability of this proposal, further studies are necessary. One should study the probability of collision among carbon clusters and that of the occur-

rence of the  $C_2$  loss of fullerene-like cages, and then to estimate the relative abundance of fullerenes. Also, the experimental studies to reveal the microscopic formation process of fullerenes are equally awaited.

#### ACKNOWLEDGMENTS

The authors would like to thank A. Oshiyama, T. Nakayama, M. Saito, and O. Sugino for the LDA program used in the present study. Some of the numerical calculations were performed on TSUBAME Grid Cluster at the Global Scientific Information and Computing Center of the Tokyo Institute of Technology. This work was partially supported by a Grant-in-Aid for Scientific Research from the Ministry of Education, Science and Culture of Japan. They also acknowledge the financial support from the Asahi Glass Foundation, Ishikawa Carbon Foundation, and the 21st Century Center of Excellence Program by Ministry of Education, Science, and Culture of Japan through the Nanometer-Scale Quantum Physics Project of the Tokyo Institute of Technology.

- 
- <sup>1</sup>H. W. Kroto, J. R. Heath, S. C. O'Brien, R. F. Curl, and R. E. Smalley, *Nature (London)* **318**, 162 (1985).
- <sup>2</sup>W. Krätschmer, L. D. Lamb, K. Fostiropoulos, and D. R. Huffman, *Nature (London)* **347**, 354 (1990).
- <sup>3</sup>S. Saito and A. Oshiyama, *Phys. Rev. Lett.* **66**, 2637 (1991).
- <sup>4</sup>J. H. Weaver, J. L. Martins, T. Komeda, Y. Chen, T. R. Ohno, G. H. Kroll, N. Troullier, R. E. Haufler, and R. E. Smalley, *Phys. Rev. Lett.* **66**, 1741 (1991).
- <sup>5</sup>A. F. Hebard, M. J. Rosseinsky, R. C. Haddon, D. W. Murphy, S. H. Glarum, T. T. M. Palstra, A. P. Ramirez, and A. R. Kortan, *Nature (London)* **350**, 600 (1991).
- <sup>6</sup>Y. Iwasa, T. Arima, R. M. Fleming, T. Siegrist, O. Zhou, R. C. Haddon, L. J. Rothberg, K. B. Lyons, H. L. Carter, Jr., A. F. Hebard, R. Tycko, G. Dabbagh, J. J. Krajewski, G. A. Thomas, and T. Yagi, *Science* **264**, 1570 (1994).
- <sup>7</sup>M. N  n  ez-Regueiro, L. Marques, J.-L. Hodeau, O. Bethoux, and M. Perroux, *Phys. Rev. Lett.* **74**, 278 (1995).
- <sup>8</sup>T. Weiske, D. K. Bohme, J. Hrusak, W. Kratschmer, and H. Schwarz, *Angew. Chem., Int. Ed. Engl.* **30**, 884 (1991).
- <sup>9</sup>K. Komatsu, M. Murata, and Y. Murata, *Science* **307**, 238 (2005).
- <sup>10</sup>K. Kikuchi, N. Nakahara, T. Wakabayashi, S. Suzuki, H. Shiroamaru, Y. Miyake, K. Saito, I. Ikemoto, M. Kainosho, and Y. Achiba, *Nature (London)* **357**, 142 (1992).
- <sup>11</sup>F. Diederich, R. Ettl, Y. Rubin, R. L. Whetten, R. Beck, M. Alvarez, S. Anz, D. Sensharma, F. Wudl, K. C. Khemani, and A. Koch, *Science* **252**, 548 (1991).
- <sup>12</sup>S. Saito and A. Oshiyama, *Phys. Rev. B* **44**, 11532 (1991).
- <sup>13</sup>S. Saito, S. I. Sawada, and N. Hamada, *Phys. Rev. B* **45**, 13845 (1992).
- <sup>14</sup>H. W. Kroto, *Nature (London)* **329**, 529 (1987).
- <sup>15</sup>S. Saito, S. I. Okada, S. Sawada, and N. Hamada, *Phys. Rev. Lett.* **75**, 685 (1995).
- <sup>16</sup>Y. Ueno and S. Saito, *Physica E (Amsterdam)* **40**, 285 (2007).
- <sup>17</sup>D. H. Parker, P. Wurz, K. Chatterjee, K. R. Lykke, J. E. Hunt, M. J. Pellin, J. C. Hemminger, D. M. Gruen, and L. M. Stock, *J. Am. Chem. Soc.* **113**, 7499 (1991).
- <sup>18</sup>A. Sesli, B.    ek, and M. Oymael, *Fullerenes, Nanotubes, Carbon Nanostruct.* **13**, 1 (2005).
- <sup>19</sup>R. E. Haufler, Y. Chai, L. P. F. Chibante, J. Conceicao, C. Fin, L. Wang, S. Maruyama, and R. E. Smalley, in *Clusters and Cluster-Assembled Materials*, edited by R. S. Averback, J. Bernbolc, and D. L. Nelson, *Mater. Res. Soc. Symp. Proc. No. 206*, (Materials Research Society, Pittsburgh, 1991), p. 627.
- <sup>20</sup>J. R. Heath, *ACS Symp. Ser.* **481**, 1 (1992).
- <sup>21</sup>T. Wakabayashi and Y. Achiba, *Chem. Phys. Lett.* **190**, 465 (1992).
- <sup>22</sup>Y. Yamaguchi and S. Maruyama, *Chem. Phys. Lett.* **286**, 336 (1998).
- <sup>23</sup>S. Maruyama and Y. Yamaguchi, *Chem. Phys. Lett.* **286**, 343 (1998).
- <sup>24</sup>S. Irle, G. Zheng, M. Elstner, and K. Morokuma, *Nano Lett.* **3**, 1657 (2003).
- <sup>25</sup>S. Irle, G. Zheng, Z. Wang, and K. Morokuma, *J. Phys. Chem. B* **110**, 14531 (2006).
- <sup>26</sup>Y. Omata, Y. Yamagami, K. Tadano, T. Miyake, and S. Saito, *Physica E (Amsterdam)* **29**, 454 (2005).
- <sup>27</sup>R. D. Johnson, C. S. Yannoni, J. Salem, G. Meijer, and D. S. Bethune, in *Clusters and Cluster-Assembled Materials (Ref. 19)*, p. 715.
- <sup>28</sup>W. Kohn and L. J. Sham, *Phys. Rev.* **140**, A1133 (1965).
- <sup>29</sup>P. Hohenberg and W. Kohn, *Phys. Rev.* **136**, B864 (1964).
- <sup>30</sup>T. Wakabayashi, D. Kasuya, H. Shiroamaru, S. Suzuki, K. Kikuchi, and Y. Achiba, *Z. Phys. D: At., Mol. Clusters* **40**, 414 (1997).
- <sup>31</sup>L. A. Bloomfield, M. E. Geusic, R. R. Freeman, and W. L. Brown, *Chem. Phys. Lett.* **121**, 33 (1985).
- <sup>32</sup>S. H. Yang, C. L. Pettiette, J. Conceicao, O. Cheshnovsky, and R. E. Smalley, *Chem. Phys. Lett.* **139**, 233 (1987).

- <sup>33</sup>Y. Achiba, C. Kittaka, T. Moriwaki, and H. Shiromaru, *Z. Phys. D: At., Mol. Clusters* **19**, 427 (1991).
- <sup>34</sup>J. Bernholc and J. C. Phillips, *Phys. Rev. B* **33**, 7395 (1986).
- <sup>35</sup>R. Car and M. Parrinello, *Phys. Rev. Lett.* **55**, 2471 (1985).
- <sup>36</sup>R. Car and M. Parrinello, *Phys. Rev. Lett.* **60**, 204 (1988).
- <sup>37</sup>G. Galli, R. M. Martin, R. Car, and M. Parrinello, *Phys. Rev. Lett.* **62**, 555 (1989).
- <sup>38</sup>G. Galli, R. M. Martin, R. Car, and M. Parrinello, *Phys. Rev. Lett.* **63**, 988 (1989).
- <sup>39</sup>N. Troullier and J. L. Martins, *Phys. Rev. B* **43**, 1993 (1991).
- <sup>40</sup>L. Kleinman and D. M. Bylander, *Phys. Rev. Lett.* **48**, 1425 (1982).
- <sup>41</sup>D. M. Ceperley and B. J. Alder, *Phys. Rev. Lett.* **45**, 566 (1980).
- <sup>42</sup>J. P. Perdew and A. Zunger, *Phys. Rev. B* **23**, 5048 (1981).
- <sup>43</sup>O. Sugino and A. Oshiyama, *Phys. Rev. Lett.* **68**, 1858 (1992).
- <sup>44</sup>C. H. Xu, C. Z. Wang, C. T. Chan, and K. M. Ho, *J. Phys.: Condens. Matter* **4**, 6047 (1992).
- <sup>45</sup>S. Nosé, *Mol. Phys.* **52**, 255 (1984).
- <sup>46</sup>S. Nosé, *J. Chem. Phys.* **81**, 511 (1984).
- <sup>47</sup>W. G. Hoover, *Phys. Rev. A* **31**, 1695 (1985).
- <sup>48</sup>E. A. Rohlfing, D. M. Cox, and A. Kaldor, *J. Chem. Phys.* **81**, 3322 (1984).
- <sup>49</sup>K. Raghavachari and J. Binkley, *J. Chem. Phys.* **87**, 2191 (1987).
- <sup>50</sup>K. Terakura, T. Hoshino, and T. Asada, in *Microclusters*, Proceedings of the First NEC Symposium, edited by S. Sugano, Y. Nishina, and S. Ohnishi (Springer, Berlin, 1987), p. 257.
- <sup>51</sup>G. von Helden, M. T. Hsu, N. Gotts, and M. T. Bowers, *J. Phys. Chem.* **97**, 8182 (1993).
- <sup>52</sup>S. C. O'Brien, J. R. Heath, R. F. Curl, and R. E. Smalley, *J. Chem. Phys.* **88**, 220 (1988).